



RESEARCH ARTICLE

MyD88 Mediates Noncytopathic Bovine Viral Diarrhea Virus Replication by Regulating Cellular Autophagy and Proliferation

Kui Wang^{1#}, Jing Yang^{1#}, Yuan Hu¹, Jie Xu¹, Yajing Chen¹, Yiyi Zhao¹, Saqib Umer², Kangfeng Jiang^{1*} and Xiaobing Li^{1*}

¹College of Veterinary Medicine, Yunnan Agricultural University, No. 452 Fengyuan Road, Panlong District, Kunming, Yunnan Province, China; ²Department of Theriogenology, University of Agriculture, Faisalabad, Pakistan

[#]These authors contributed equally to this study

*Corresponding author: kangfengjiang@ynau.edu.cn (KJ); xiaobingli@yeah.net (XL)

ARTICLE HISTORY (24-854)

Received: December 27, 2024
Revised: February 25, 2025
Accepted: February 26, 2025
Published online: March 28, 2025

Key words:

Autophagy
Cell Proliferation
MyD88
NCP BVDV
Virus Replication

ABSTRACT

Bovine viral diarrhea virus (BVDV) is classified into cytopathic (CP) and noncytopathic (NCP) types. Previous studies confirmed that NCP BVDV infection is the main cause of persistent infection and immune suppression in cattle, and its molecular mechanism of using host biological processes to evade immunity remains unclear. We initially examined the replication of the AV303 strain (NCP BVDV) in MDBK cells at different time points. Proteomic analysis at the peak replication time point revealed that the TLR signaling pathway and the adaptor protein Myeloid differentiation factor 88 (MyD88) were upregulated. Subsequently, we found that AV303 infection initiated autophagy but had degradation barriers, meanwhile the proliferation rate of MDBK cells increased. After knocking down MyD88, the cell proliferation rate was restored, and autophagy flow was activated utterly. Mechanistically, AV303 regulated cell proliferation by promoting ERK1/2 and Akt/mTOR, and both activities were inhibited after MyD88 is knocked down. The activity of MyD88 affected the degradation stage of autophagic flux. Treatment with autophagy agonists inhibits AV303 replication, whereas autophagy inhibitors enhance its replication. This study demonstrates that the activity of MyD88 mediated by the AV303 strain can regulate host cell autophagy and proliferation, creating advantageous conditions for its replication. This study identifies a novel mechanism in host-NCP BVDV interaction and highlights the potential of MyD88 as a target for anti-NCP BVDV drug development.

To Cite This Article: Wang K, Yang J, Y H, Xu J, Chen Y, Zhao Y, Umer S, Jiang K, Li X, 2025. MyD88 mediates noncytopathic bovine viral diarrhea virus replication by regulating cellular autophagy and proliferation. *Pak Vet J*, 45(1): 112-123. <http://dx.doi.org/10.29261/pakvetj/2025.130>

INTRODUCTION

As non-cellular organisms, viruses rely on their hosts for energy and suitable environmental conditions necessary for survival and reproduction. As foreign entities, they are often targeted and eliminated by various defense systems of the host. Consequently, viruses must continually evolve sophisticated strategies to evade host defenses. Bovine viral diarrhea virus (BVDV) is a member of the family *Flaviviridae* and the genus *Pestivirus*. It is a single-stranded RNA virus that causes high fever, diarrhea, and damage to the mucous membranes of the esophagus and digestive tract in cattle, which results in significant economic losses to the livestock industry. BVDV is classified as cytopathic (CP) or non-cytopathic (NCP) on the basis of the two different phenotypes (biotypes) exhibited in cell culture (Lindberg

and Houe, 2005). NCP BVDV can cause fetal persistent infection in cows during pregnancy, which is also a major cause of immune suppression in cattle (Peterhans *et al.*, 2010). Additionally, CP BVDV biotypes are result of mutation of NCP BVDV (Duan *et al.*, 2020).

Autophagy is a crucial and evolutionarily conserved cellular mechanism that facilitates the encapsulation of damaged proteins, organelles, and microorganisms within double-membraned autophagic vesicles for subsequent lysosomal degradation (Mathew *et al.*, 2007; Parzych and Kliensky, 2014; Zhang *et al.*, 2020). This process enables cells to eliminate senescent organelles and damaged structures and reuse them, especially under stressful conditions such as cellular starvation, malnutrition, or pathogen invasion, autophagy is activated to cope with adverse environmental stress. Many viruses were proved to regulate or be affected by autophagy during replication.

The role of autophagy in essential biological functions, including innate immunity and inflammation, has been well documented (Xu *et al.*, 2008). Numerous viruses, such as African swine fever virus (ASFV), foot-and-mouth disease virus (FMDV), pseudorabies virus (PRV), and Japanese encephalitis virus (JEV), are capable of initiating host autophagy following infection (Jiang *et al.*, 2022; Liu *et al.*, 2022). The interaction between autophagy and viruses has led to different outcomes, with some studies finding that activation of autophagy promotes viral replication, as observed with Newcastle disease virus (NDV) (Gong *et al.*, 2022) and JEV (Li *et al.*, 2012). In contrast, the activation of autophagy inhibits the replication of viruses, such as herpes simplex virus (HSV) (Rubio and Mohr, 2019). Several viruses in the *Flaviviridae* family have been shown to induce autophagy both *in vitro* and *in vivo*. In addition, two biological types of BVDV can activate autophagy (Rajput *et al.*, 2017), but the underlying mechanisms and dynamics remain incompletely understood. Like other viruses, BVDV has developed strategies that allow it to evade host immune responses as it continues to spread and infect hosts (Pang *et al.*, 2023); however, it is still uncertain whether autophagy is dominant, even though there are studies shown that BVDV induced autophagy (Fu *et al.*, 2014).

Cell proliferation results from cell growth and division, which are primarily controlled by the cell cycle (Ogrodnik, 2021). After cell proliferation, it can create replication conditions for viruses. For example, human papillomavirus (HPV) interferes with host cell cycle regulation by expressing specific proteins, thereby promoting cell proliferation and creating an environment conducive to virus proliferation (McCance, 2005). HIV utilizes the polymerase and nucleotides of host cells for genome replication (Spence *et al.*, 1995). In addition, certain viruses, such as the EB virus, can activate the proliferation signaling pathway of host cells, leading to latent or persistent infection within the host's body (Guasparri *et al.*, 2008; Luo *et al.*, 2021). Therefore, we assume that the NCP BVDV also has evolved with similar abilities. We investigated whether NCP BVDV regulates host cells by detecting the activity of the classical cell proliferation signaling pathways Akt/mTOR and MAPK/ERK 1/2.

Previous omics studies have provided insights into the changes in life processes within the host following viral infection (Ma *et al.*, 2022; Mirosław *et al.*, 2022). However, the mechanisms of interaction between BVDV and its host are still poorly understood. Our preliminary omics results identified a potential association between NCP BVDV and the TLR7-MyD88 signaling pathway. Toll-like receptors (TLRs), as pattern recognition receptors, quickly identify pathogen characteristics and initiate the signaling cascades involved in immune defense (Delgado and Deretic, 2009; Urcuqui-Inchima *et al.*, 2017). There is substantial evidence suggesting a significant association between TLRs and the process of autophagy following various infections (Thompson and Iwasaki, 2008). For example, single-stranded RNA (ssRNA) and other TLR7 agonists are recognized as potent inducers of autophagy (Iwasaki, 2007). MyD88 is a bridging protein that activates all TLR pathways except TLR3, many studies indicate that MyD88 activity

is essential for autophagy (Shi and Kehrl, 2008; Siracusano *et al.*, 2016; Wang *et al.*, 2018). However, reports regarding its role in the context of pathogenic infections have been inconsistent. It can act both as an activator of autophagy (Song *et al.*, 2024) and as a target for inhibiting it (Kader *et al.*, 2017). Therefore, we want to know whether MyD88 plays an important role in autophagy of BVDV infected cells and its impact on BVDV replication in cells. Additionally, MyD88 has been shown to target signaling pathways related to immune cell and cancer cell proliferation (Chang *et al.*, 2013; Salcedo *et al.*, 2013; Liu *et al.*, 2020), which prompted us to study its involvement in the cell proliferation influenced by NCP BVDV.

In this study, we reported the relationship between AV303 (NCP type) replication and MyD88 mediated cellular autophagy and proliferation and identified a novel immune evasion mechanism of NCP BVDV and the important role of MyD88 in NCP BVDV replication.

MATERIALS AND METHODS

Cells and viruses: MDBK cells were stored in our laboratory and cultured in RPMI-1640 containing 10% fetal bovine serum (cell-box AUS-01S-02-S). The AV303 strain (NCP type) was purchased from the China Veterinary Culture Collection Center and preserved by our laboratory.

Proteomic sequencing and analysis: The protein was extracted using the SDT lysis method (4% (w/v) SDS, 100 mM Tris/HCl pH 7.6, 0.1 M DTT) and then quantified using the BCA method. An appropriate amount of protein was extracted from each sample, and the filter-aided protein preparation (FASP) method was used for trypsin hydrolysis. Then 18 cartridges were used to desalinate the peptide segments. After freeze-drying, 40 µL of 0.1% formic acid solution was added for reconstitution, and the peptide segments (OD280) were quantified. Peptide segments (100 µg) from each sample were labeled according to the instructions of the Thermo TMT labeling kit. Each group contained 3 biological replicates, for a total of 6 samples. The labeled peptides were fractionated with a high-pH reversed-phase peptide fractionation kit (Thermo Scientific). The dried peptide mixture was reconstructed and adjusted to acidic pH using a 0.1% TFA solution and loaded onto an equilibrated, high-pH, reversed-phase fractionation spin column. Peptides were bound to the hydrophobic resin under aqueous conditions and desalted by washing the column with water using low-speed centrifugation. A step gradient of increasing acetonitrile concentrations in a volatile high-pH elution solution is then applied to the columns to elute bound peptides into 10 different fractions collected by centrifugation. The collected fractions were desalted on C18 cartridges (Empore™ SPE cartridges C18 (standard density), bed I.D. 7 mm, Volume 3 ml, Sigma) and concentrated by vacuum centrifugation. Each sample was separated via an easy nLC HPLC system with a nanoliter flow rate. The chromatographic column was equilibrated with 95% A solution, and the sample was loaded onto a loading column (Thermo Scientific Acclaim PepMap100, 100 µm * 2 cm, nanoViper C18) via an automatic

sampler. The sample was then separated on an analytical column (Thermo Scientific EASY column, 10 cm, ID 75 μm , 3 μm , C18-A2) at a flow rate of 300 nL/min. After chromatographic separation, the sample was analyzed via mass spectrometry using a Q Exactive mass spectrometer. The detection method was positive ion mode, with a scanning range of 300–1800m/z for parent ions, a primary mass spectrometry resolution of 70000 at 200m/z, an automatic gain control (AGC) target of 1e6, a maximum internal time (IT) of 50ms, and a dynamic exclusion time of 60.0s. The mass-charge ratios of the peptides and peptide fragments were determined using the following method: 20 fragment spectra (MS2 scan) were collected after each full scan, with an MS2 activation HCD isolation window of 2m/z, a secondary mass spectrometry resolution of 17500 at 200m/z, a normalized collision energy of 30 eV, and an underwater energy of 0.1%. The inventory identification and quantitative analysis were carried out using the software programs Mascot 2.2 and Proteome Discoverer 1.4, which involved techniques such as principal component analysis (PCA), partial least squares discriminant analysis (PLS-DA), univariate analysis, and pathway analysis. For the metabolomics analysis, both multivariate statistical methods, including PCA and PLS-DA, and univariate tests—such as the Student's t-test, Mann–Whitney–Wilcoxon U test, analysis of variance (ANOVA), and correlation analysis—were performed.

Cell proliferation assay: Adherent cells and cell suspensions after virus infection were treated using the BeyoClick™ EdU Cell Proliferation Kit with Alexa Fluor 594 and observed using a confocal fluorescence microscope (Ningbo Sunny RX50RFL) and flow cytometry (Thermo CytoFLEX).

Quantitative real-time polymerase chain reaction: The cells were lysed using RNAiso Plus (Takara, Kyoto, Japan). Cells' RNA was extracted using reagents, including chloroform, isopropanol, and absolute ethanol, with shaking and centrifugation according to the manufacturer's protocol. One percent gel electrophoresis was used to verify the integrity of the RNA, after which the RNA was reverse transcribed to cDNA using EasyScript® One-Step gDNA Removal and cDNA Synthesis SuperMix. The quantitative detection of mRNA was performed using a real-time PCR instrument (qTOWER3G, Analytik Jena) with a program set at 94 °C/5 min, 94 °C/30 s \rightarrow 60 °C/30 s \times 35 cycles. The following primers (Table 1A) were designed in NCBI (National Center for Biotechnology Information) and Primer3 Input 4.0 and synthesized by Sango, and detection was performed using MCE (MedChemExpress) qPCR Master Mix and YBR Green qPCR Master Mix (Universal).

Table 1: RT-qPCR sequence of primer

Gene	Sequence(5'–3')
β -actin:	Forward: GCAGGAGTACGATGAGTCCG Revers: GCAGGAGTACGATGAGTCCG
BVDV	Forward: GCGATCCGTCTCCGTCTCC Revers: ACGCCCGTAGCCGTAGCC
MyD88	Forward: ACCAACCCCTGCACCCAGAAC Revers: ACCAACCCCTGCACCCAGAAC

Autophagic flux assay: The cells were seeded onto slides and transfected at a density of 50–70% using the lentiviral vector Mchery EGFP-LC, purchased from HanBio Technology (Shanghai, China). The principle was based on the stability of two fluorescent environments with different pH values. When autophagosomes are formed both green and red fluorescence can be detected, and autophagosomes can be observed as yellow fluorescence. However, when autophagosomes form in an acidic pH, GFP fluorescence is quenched, only red fluorescence can be observed. Therefore, when both red dot fluorescence (mCherry) and green dot fluorescence (GFP) increase, this indicates an increase in autophagic flux.

Western blotting: Adherent cells were lysed with RIPA protein lysis buffer (Solarbio), and their concentrations were determined and normalized using a BCA protein quantification kit (Shanghai Yaenzym Biotechnology). The extracted protein was added to the sample buffer in equal proportions, and the SDS–PAGE mixture was prepared for electrophoresis with a Bio-Rad electrophoresis-transfer device and a PVDF membrane for transfer. The membrane was subsequently placed in commercial rapid blocking solution (Shanghai Yazyme) for 15 min, after which the primary antibodies were incubated at 4 °C overnight. The following primary antibodies were used: BVDV E2 mAb (rabbit, VMRD P130715), ATG5 (rabbit, Abcam Cat#ab228668), LC3B (rabbit, Abcam Cat#ab48394), nucleoprin p62 (rabbit, Abcam Cat#ab96134), Akt (rabbit, Abcam Cat#ab8805), Akt (S473) (rabbit, Abcam Cat#ab81283), mTOR (rabbit, Abcam Cat#ab32028), mTOR (phospho S2448) (rabbit, Abcam Cat#ab109268), MyD88 (rabbit, Proteintech Cat#23230-1-AP), TLR7 (rabbit, cst Cat#5632), ERK1/2 (rabbit, Abclonal). The samples were subsequently rinsed with TBST 3–5 times for 10 min and incubated with the secondary antibody at room temperature for 1–2h after aspiration. The secondary antibodies used were goat anti-rabbit IgG H&L (Bioss, bs-80295G-HRP) and goat anti-mouse IgG H&L (Bioss, bs-0296G-HRP).

Immunofluorescence: After cells are infected by viruses, the cells were fixed with 4% paraformaldehyde, permeabilized with 0.2% Triton X-100 and PBST (PBS + 0.1% Twenn20) supplemented with 1% BSA, and incubated with the Alexa Fluor-conjugated primary antibody in a wet cassette for 1 h, followed by incubation with the secondary antibody for 1h at room temperature in the dark, and incubation for 5–10 min with the nuclear dye Hoechst. Mounting medium was used to mount and observe the samples under a fluorescence microscope.

Transfection by electroporation: RNA oligonucleotides were synthesized by GenePharma. The sequences for the Si MyD88 oligonucleotides are as follows (5' to 3'): Sense: CUUGACGAAUACCUGCAATT; Antisense: UUGCAGGUAUUCGUCAGAGTT. The sequences for the NC (negative control) oligonucleotides were as follows: sense: UUCUCCGAACGUCACGUTT; antisense: ACGUGACACGUUCGGAGAATT. Cells were routinely passaged and were cultivated to 80% confluence. Next, the cells were trypsinized, centrifuged, and washed three times with serum-free medium. The cells were then resuspended

in the electrophoresis buffer. For electroporation, 10 μ L of NC or Si MyD88 plasmids were added to each 200 μ L of cells suspension, which was then transferred into an electrode cup. The electroporation instrument was set to deliver a 900V square wave. After electroporation, the cells suspensions were transferred to a six-well cells culture plate and stabilized by the addition of 5% fetal bovine serum. The cells were then incubated for 6 hours.

Transmission electron microscopy: Discard the culture medium from the cells culture well plate (cells density not greater than 80%) then trypsin and medium were added to obtain a cells suspension, which was aspirated into a centrifuge tube and centrifuged at low speed (no more than 3000 rpm) for approximately 3–5 min. The supernatant was discarded, electron microscope fixative solution was added (the fixative solution needed to be restored to room temperature in advance), and the cells mass was removed and resuspended. The mixture was fixed at room temperature in the dark for 30min, transferred to 4°C for storage, and transferred to Wuhan Saiwei Biotechnology Co., Ltd., for imaging.

Statistical analysis: GraphPad Prism version 8.0 (GraphPad software) was used for statistical analysis. All data are presented as means \pm SDs, and $P < 0.05$ was considered to indicate a statistically significant difference. All the samples were analyzed in triplicate. Proteomics uses Fisher's exact test to compare the distribution of various GO classifications (or KEGG pathways or domains) in the target protein set and overall protein set and performs GO annotation or KEGG pathway enrichment analysis on the target protein set.

RESULTS

NCP BVDV infection activates the TLR7–MyD88 signaling pathway: RT–qPCR detection of the copy number of AV303 at different time points and the generation of growth curves revealed that the highest replication rate was observed between 36 and 48hpi (Fig. 1A). Immunofluorescence detection of MDBK cells infected with the AV303 strain at 48 hpi was then performed, and the amount of viral mRNA in the infected cells was determined. The results revealed that the virus successfully infected the cells with high infection efficiency (Fig. 1B). Based on the above results, we selected 48hpi for proteomics sample collection. Significantly differentially expressed proteins, including MyD88 (Fig. 1C), were identified among the protein entries with significant differences. Western blotting and qRT–PCR confirmed the significant upregulation of MyD88 protein and mRNA levels, as well as activation of the TLR7 pathway (Fig. 1D). The functional annotation results of the differentially expressed proteins revealed significant differences in protein biological processes between the upregulated and downregulated MDBK cells after infection. The important differentially expressed terms included extracellular organelles, drug metabolic processes, small-molecule metabolic processes, oxidation reduction processes, the mitochondrial inner membrane, and the organelle inner membrane (Fig. 1E). In the control vs. NCP proteomics, KEGG-identified differentially

expressed proteins, including those associated with the pentose phase pathway, the Toll and Imd signaling pathway, the AMPK signaling pathway, the MAPK signaling pathway, and the Toll-like receptor signaling pathway, were significantly upregulated. The significantly downregulated genes were involved in geraniol degradation, tryptophan metabolism, complex and coagulation cascades, the hematopoietic cells lineage, the integrated immune network for IgA production, and the production of cells adhesion molecules and steroid biosynthesis (Fig. 1F).

MyD88 mediates AV303-induced autophagy in MDBK cells: To detect the autophagy activity of MDBK cells infected with the AV303 virus strain, we examined the expression of autophagy-related proteins, including the autophagosome marker LC3, the autophagy-related gene ATG5, and the autolysosome-related protein SQSTM1 (p62). Compared with the control group, the ratio of LC3II/LC3I and the expression level of ATG5 were significantly greater in the infected group. It is worth noting that as a substrate of autophagosomes, the expression activity of p62 also showed significant upregulation (Fig. 2A), indicating that the fusion of autolysosomes may be hindered. The transmission electron microscopy results revealed a significant increase in the number of autophagosomes (autolysosomes) in the infected group (Fig. 2B). In addition, the dual color tag (mCherry GFP-LC3) fused with LC3 was further used to detect autophagy flux revealed the number of autophagosomes (autolysosomes) in the infected group was not statistically significant compared to the control group. (Fig. 2C). The MyD88 gene was knocked down by siRNA with high efficiency (Fig. 2D). We subsequently infected MyD88-knockdown cells with AV303 and found that the expression levels of LC3 and ATG5 were significantly decreased following MyD88 knockdown, whereas the expression of p62 was upregulated compared to the control group, although the difference was not statistically significant. (Fig. 2E). The TEM results further showed a significant increase in the number of autophagosomes/autolysosomes between the MyD88 knockout group and the control group after infection (Fig. 2F). In addition, the mCherry-GFP-LC3 autophagy fluorescence system showed that autophagy flow was fully activated after MyD88 knockdown (Fig. 2G).

MyD88 activity promotes cell proliferation: We investigated the potential association between cellular activities and MyD88 and hypothesized that viruses may manipulate cellular proliferation to facilitate their replication. Therefore, we examined postinfection cellular proliferative activity. Immunofluorescence and flow cytometry demonstrated the enhancement of cell proliferation signals after infection (Fig. 3A, 3B). Cell proliferation refers to the vital process of cell division, which is regulated by extracellular signals intracellular signals (such as the cell proliferation signaling pathways Akt/mTOR (Cho *et al.*, 2009) and MAPK/ERK(Nojima *et al.*, 2008)), and environmental factors (such as nutrients and oxygen levels). Consequently, we examined the signaling pathways that regulate cell growth and proliferation and the activities of Akt/mTOR and ERK1/2

pathways. The results revealed that the phosphorylation of Akt/mTOR and ERK1/2 increased (Fig. 3C). These findings confirmed that AV303 can promote cell proliferation by activating the extracellular signaling pathway. Furthermore, we examined whether knocking down MyD88 resulted in any changes, and the results revealed that MyD88-knockdown cells exhibited reduced proliferative activity after infection with AV303 (Fig. 3D, 3E); On the signaling pathway, the activity of Akt/mTOR and ERK1/2 in MyD88 knockdown cells is inhibited compared to non-knockdown cells, and the activation level is limited after infection with AV303. (Fig. 3F). Therefore, we confirmed that the activity of MyD88 affects cell proliferation, which is related to the activation of the Akt/mTOR and ERK1/2 pathways.

The autophagic activity of MDBK regulates the replication of AV303: Based on these findings, we speculated that the replication of NCP BVDV is related

to the autophagic activity of MDBK. Therefore, we treated the cells with the autophagy activator rapamycin and the autophagy inhibitor MHY1485 and then infected them with the virus. The western blotting results revealed that the Akt/mTOR pathway was activated by MHY1485, inhibited by rapamycin (Fig. 4A), and regulated the autophagy induced by AV303 infection (Fig. 4B). Moreover, the use of both rapamycin and MHY1485 for viral infection affected the replication of the virus. The accumulation of NCP BVDV mRNA and the protein expression of E2 were inhibited by rapamycin but promoted by MHY1485 (Fig. 4C, 4D). The immunofluorescence results of BVDV E2 further showed that the replication ability of AV303 was affected by changes in autophagy activity. As shown in Fig. 4E, the fluorescence signal of BVDV E2 is enhanced in cells treated with autophagy inhibitors and weakened in cells treated with autophagy agonists.

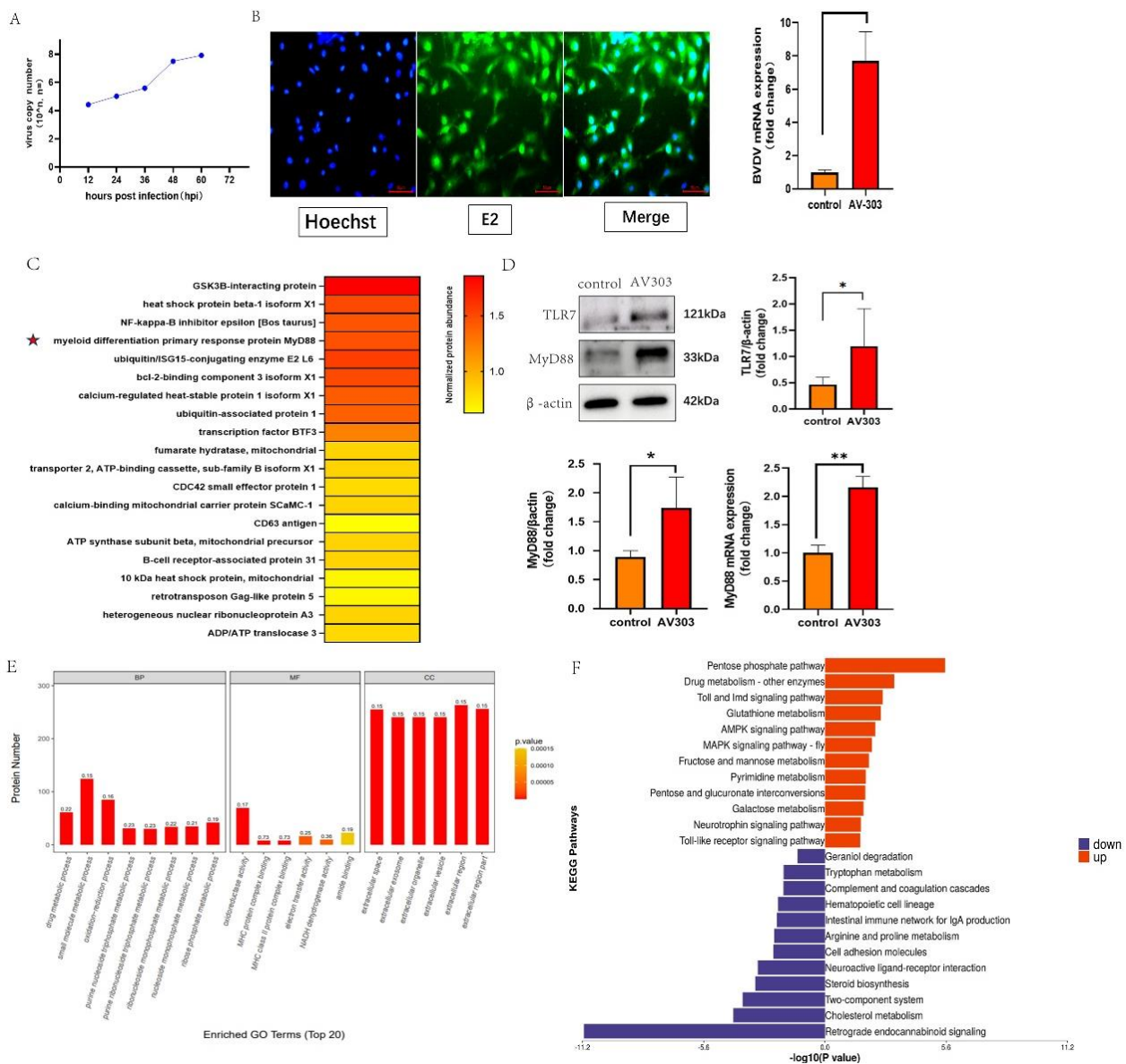


Fig. 1: AV303 strain activates TLR7-MyD88 pathway. (A) AV303 growth curve; (B) Immunofluorescence results of E2 structural protein after viral infection in cells; (C) Heat map of significantly upregulated and downregulated differentially expressed proteins (top 10) (p value < 0.05); (D) Validation of TLR7-MyD88 after AV303 infection; (E) GO project analysis of differential proteins; (F) KEGG project analysis of differential expression pathways. The data are expressed as mean ± SEM. Statistical significance was assessed using the Student's t-test. *P < 0.05, **P < 0.01. All data comes from three independent repeated experiments.

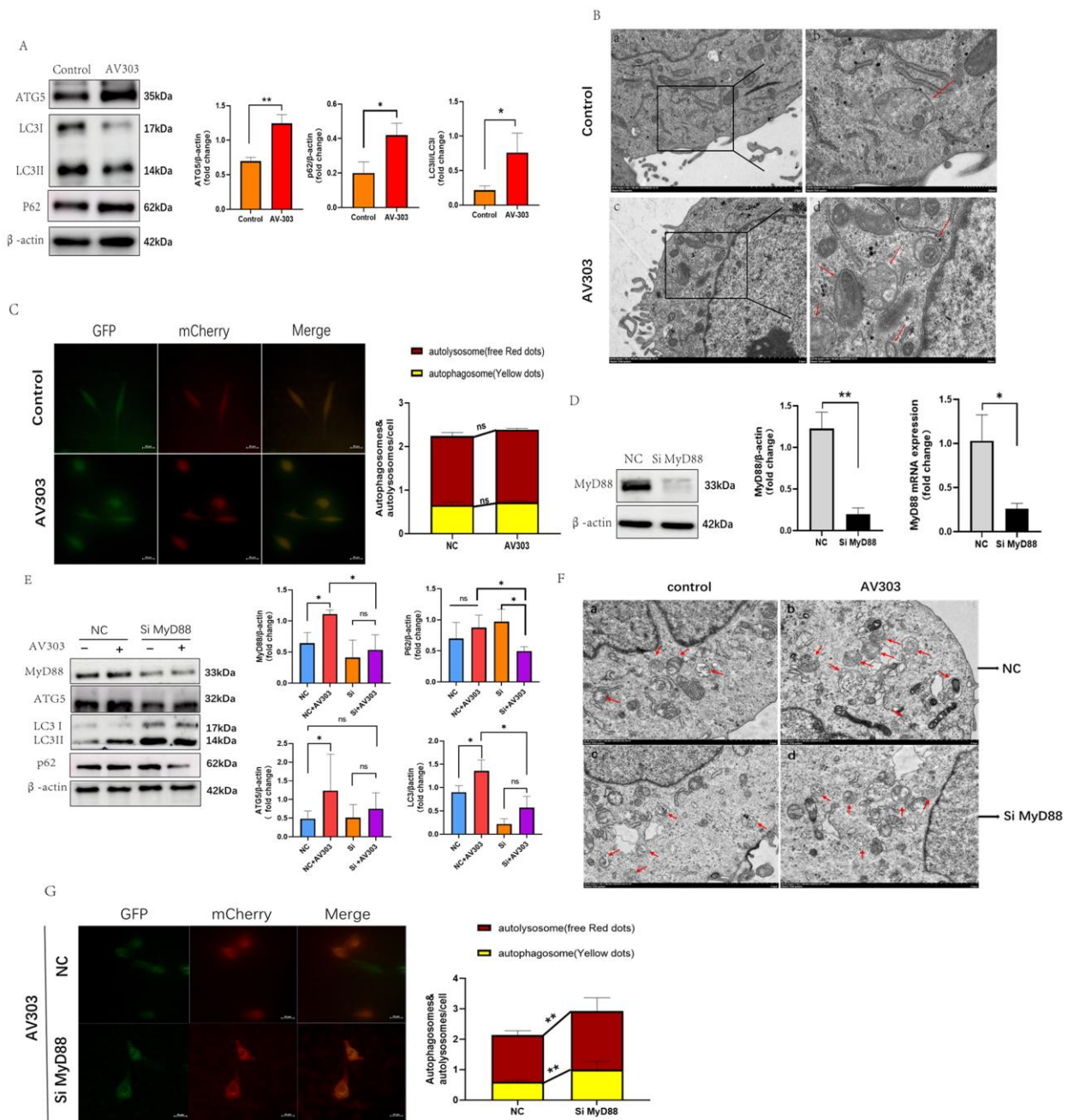


Fig. 2: The relationship between AV303 induced autophagy and MyD88. (A) Protein immunoblotting analysis of cell lysate obtained after viral infection, expression of representative proteins indicating autophagic activity; (B) Transmission electron microscopy (TEM) to examine the formation of autophagosomes (autolysosomes), a and b were the control group, where b was the high-magnification group, and c, d were the infection group, where d was the high-magnification group; (C) Detection of autophagosomes and autolysosomes using fluorescence microscopy; (D) Efficiency detection of Si MyD88 transfection into MDBK cells; (E) Detection of autophagy activity, expression of representative proteins indicating autophagic activity; (F) Transmission electron microscopy (TEM) to examine the formation of autophagosomes (lysosomes). a is the NC uninfected group, b is the NC infected group, c is the Si MyD88 uninfected group, and d is the Si MyD88 infected group. (G) Fluorescence microscopy examination of autophagosomes and autolysosomes; H and E X400. The data are expressed as mean \pm SEM. Statistical significance was assessed using the Student's t-test. * $P < 0.05$, ** $P < 0.01$. All data comes from three independent repeated experiments.

MyD88 activity mediates AV303 replication: These results indicate that the replication of AV303 is closely related to the autophagy and proliferation of MDBK. To directly understand the relationship between MyD88 activity and AV303 replication, we simultaneously detected the mRNA levels of MyD88 knockdown and BVDV. BVDV mRNA levels exhibited a MyD88-dependent trend (Fig. 5A, B). In addition, western blotting and immunofluorescence revealed a significant decrease in BVDV E2 protein expression after MyD88 knockdown compared with the NC group (Fig. 5C, D).

DISCUSSION

The fact is that viruses have evolved various mechanisms to respond to host immunity, while the molecular mechanisms of immune evasion vary among different viruses. While many potential mechanisms of BVDV immune escape have been elucidated, the mechanisms underlying virus replication, development, and host interaction remain to be explored. The initial omics results showed more upregulated immune-related DEPs than downregulated ones, suggesting that BVDV

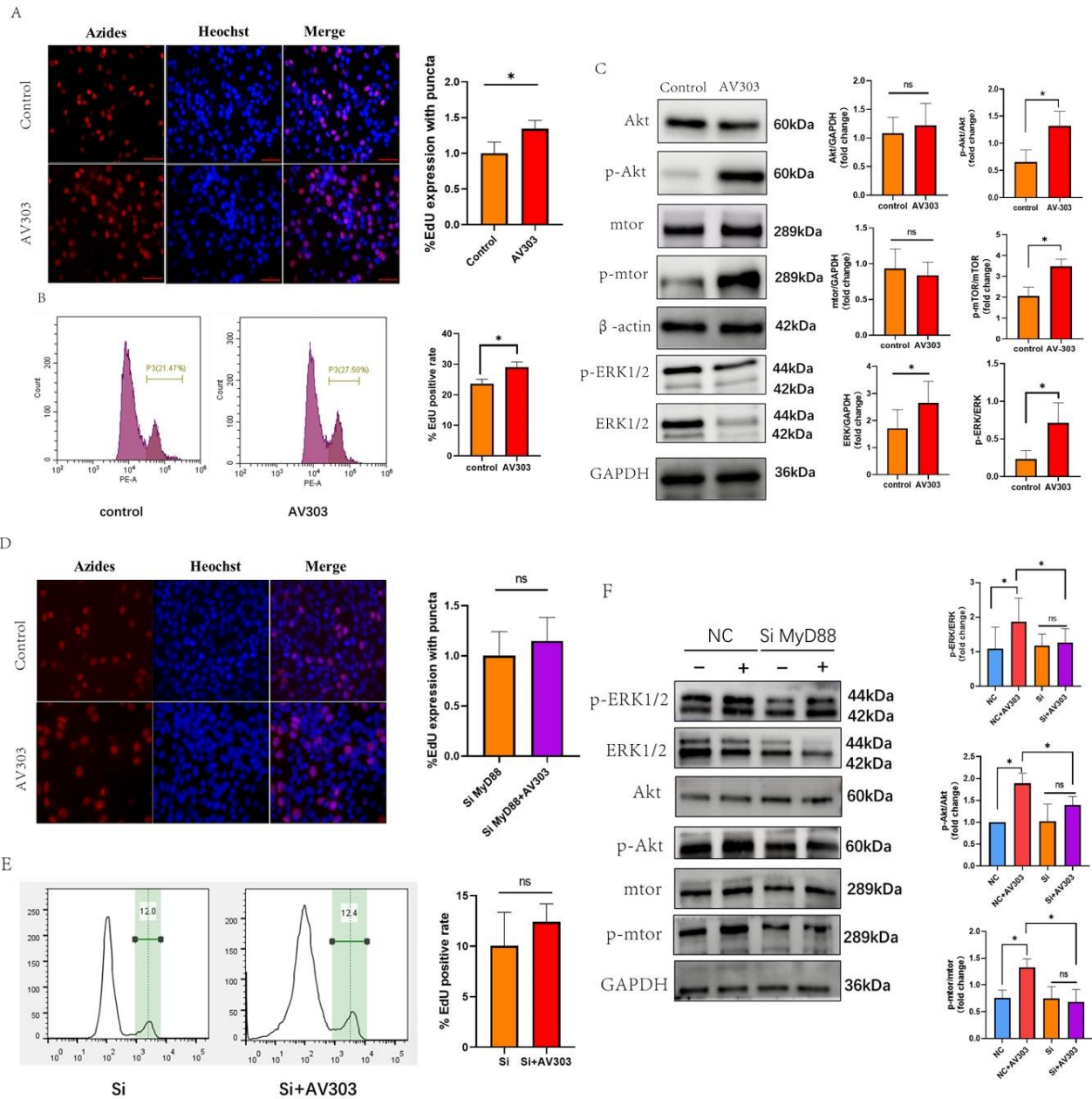


Fig. 3: The effect of MyD88 induced autophagy on cell proliferation. (A) Fluorescence microscopy detection of EdU fluorescence signal in cell proliferation after AV303 infection; (B) Flow cytometry quantitative analysis of EdU cell proliferation signal after AV303 infection; (C) Protein immunoblotting detection of changes in cell proliferation pathway activity after AV303 infection; (D) MDBK cells knocked down by Si MyD88 were infected with AV303, and the EdU fluorescence signal during cell proliferation was detected by fluorescence microscopy; (E) MDBK cells knocked down by Si MyD88 were infected with AV303, and the EdU fluorescence signal during cell proliferation was analyzed by flow cytometry; (F) Protein immunoblotting detection of the effect of MyD88 knockdown on the proliferation pathway activity of virus-infected cells. The data are expressed as mean \pm SEM. Statistical significance was assessed using the Student's t-test. * $P < 0.05$, ** $P < 0.01$. All data comes from three independent repeated experiments.

suppresses the host immune system to aid its survival during infection. However, during the metabolic process, the number of upregulated DEPs was significantly greater than that of downregulated DEPs, indicating that BVDV may hijack host metabolism during replication. Most viruses primarily inhibit IFN-I replication as their main strategy to evade host immunity such as SARS-CoV-2 (Wang *et al.*, 2021), African swine fever virus (Li *et al.*, 2021), porcine epidemic diarrhea virus (Zheng *et al.*, 2021). In addition, certain viruses have evolved more sophisticated mechanisms to further adapt to the host's immune response. The smallpox virus, for instance, encodes a Bcl-2-like protein that prevents host

cell apoptosis (Senkevich *et al.*, 2021). The influenza virus employs antigenic drift and shift, continually altering its surface antigens, thus hindering the host immune system's ability to recognize and respond effectively (Zost *et al.*, 2019). Additionally, HSV reduce NK cell recognition of infected cells by encoding proteins that interfere with MHC I molecule expression (Tognarelli *et al.*, 2019). Some viruses, such as the HPV (Steinbach and Riemer, 2018), are unable to fully escape the host's immune defenses. Instead, they persist within the host overtime through a symbiotic relationship with the immune system, maintaining a chronic presence without triggering an overt immune response.

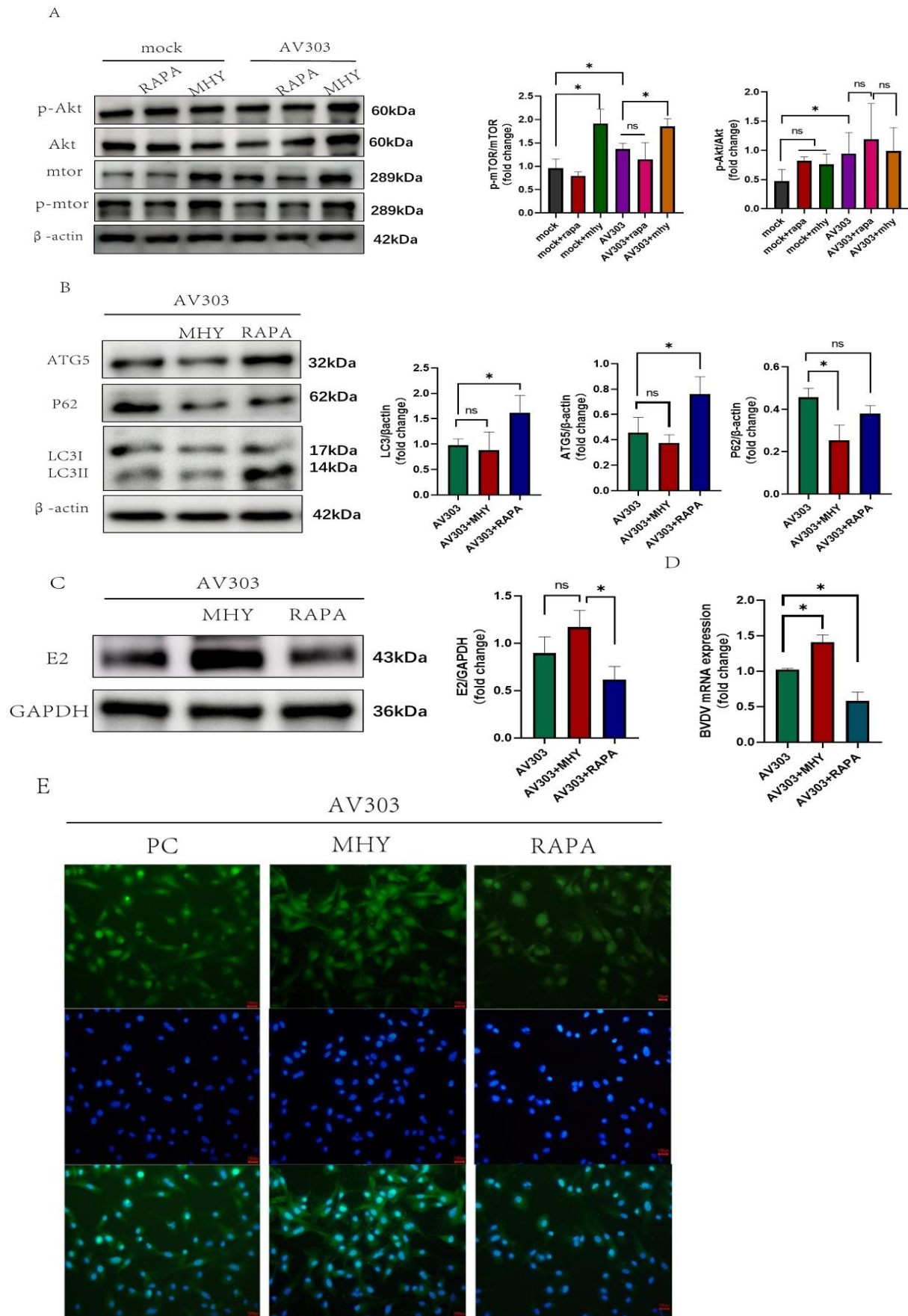


Fig. 4: The effect of drugs on autophagy induced by AV303. (A) Western blot analysis of the effects of autophagy activators and inhibitors before and after viral infection; (B) Western blot detection of the regulation of autophagy by autophagy activators and inhibitors before and after viral infection; (C) Protein immunoblotting detection of the effects of autophagy activators and inhibitors on the expression of AV303 E2 protein; (D) Immunofluorescence detection of the effects of autophagy activators and inhibitors on the expression of AV303 E2 protein; (E) Immunofluorescence detection of the effects of rapamycin and MHY-1485 on the replication of AV303 virus. The data are expressed as mean \pm SEM. Statistical significance was assessed using the Student's t-test. * $P < 0.05$, ** $P < 0.01$. All data comes from three independent repeated experiments.

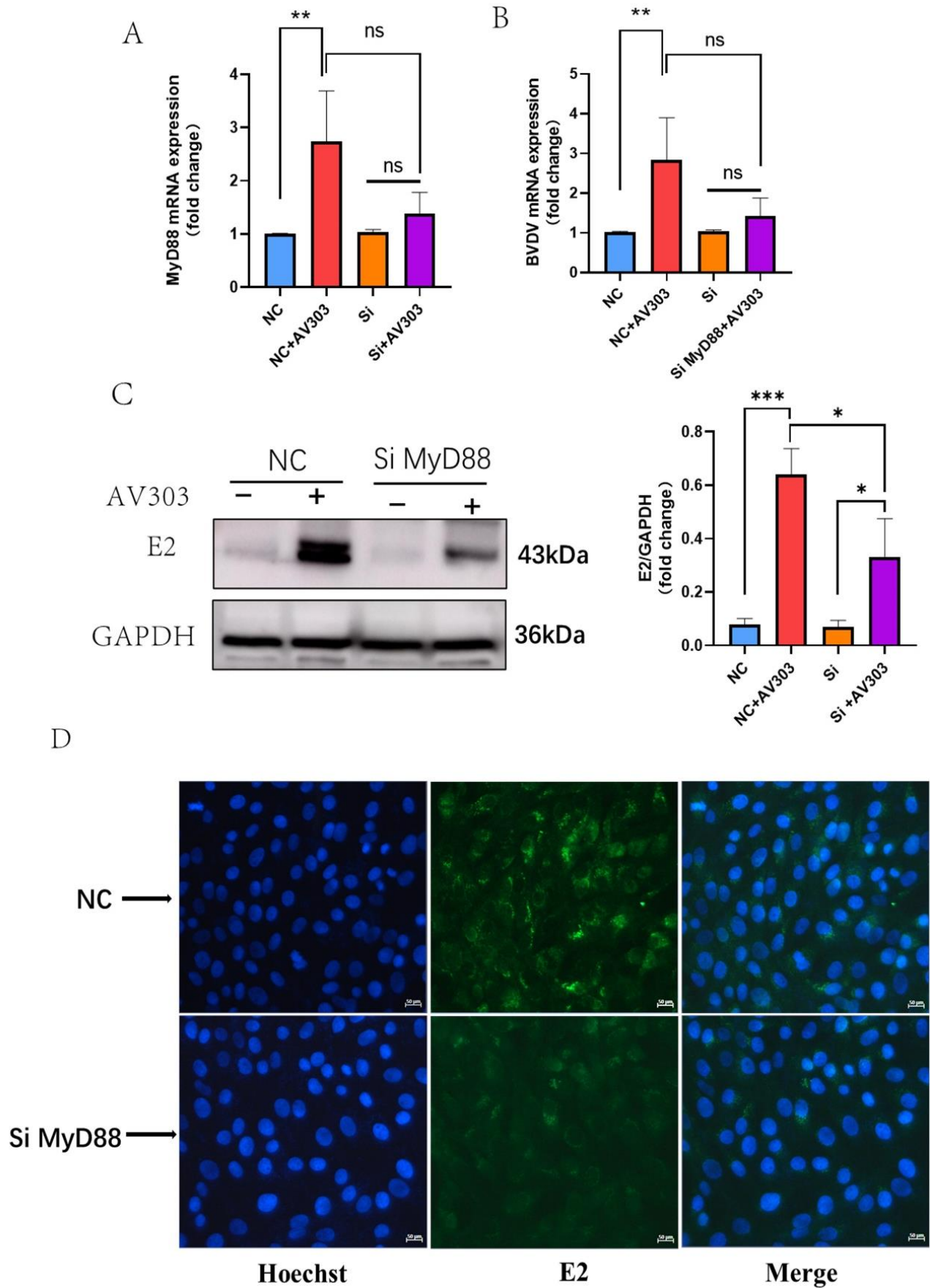


Fig. 5: The effect of MyD88 activity on AV303. (A) Protein immunoblotting detection of the effect of MyD88 knockdown on TLR7 expression; (B) RT qPCR detection of the effect of MyD88 knockdown on the accumulation of IRF3, IRF7, and IFN I mRNA; (C) Protein immunoblotting detection of the effect of MyD88 knockdown on the expression of IRF3 and IRF7 proteins; (A) RT qPCR detection of changes in MyD88 mRNA; (B) RT qPCR detection of changes in BVDV mRNA. (C) Protein immunoblotting detection of changes in BVDV E2 protein expression; (D) Immunofluorescence detection of changes in BVDV E2 protein expression. The data are expressed as mean \pm SEM. Statistical significance was assessed using the Student's *t*-test. * $P < 0.05$, ** $P < 0.01$. All data comes from three independent repeated experiments.

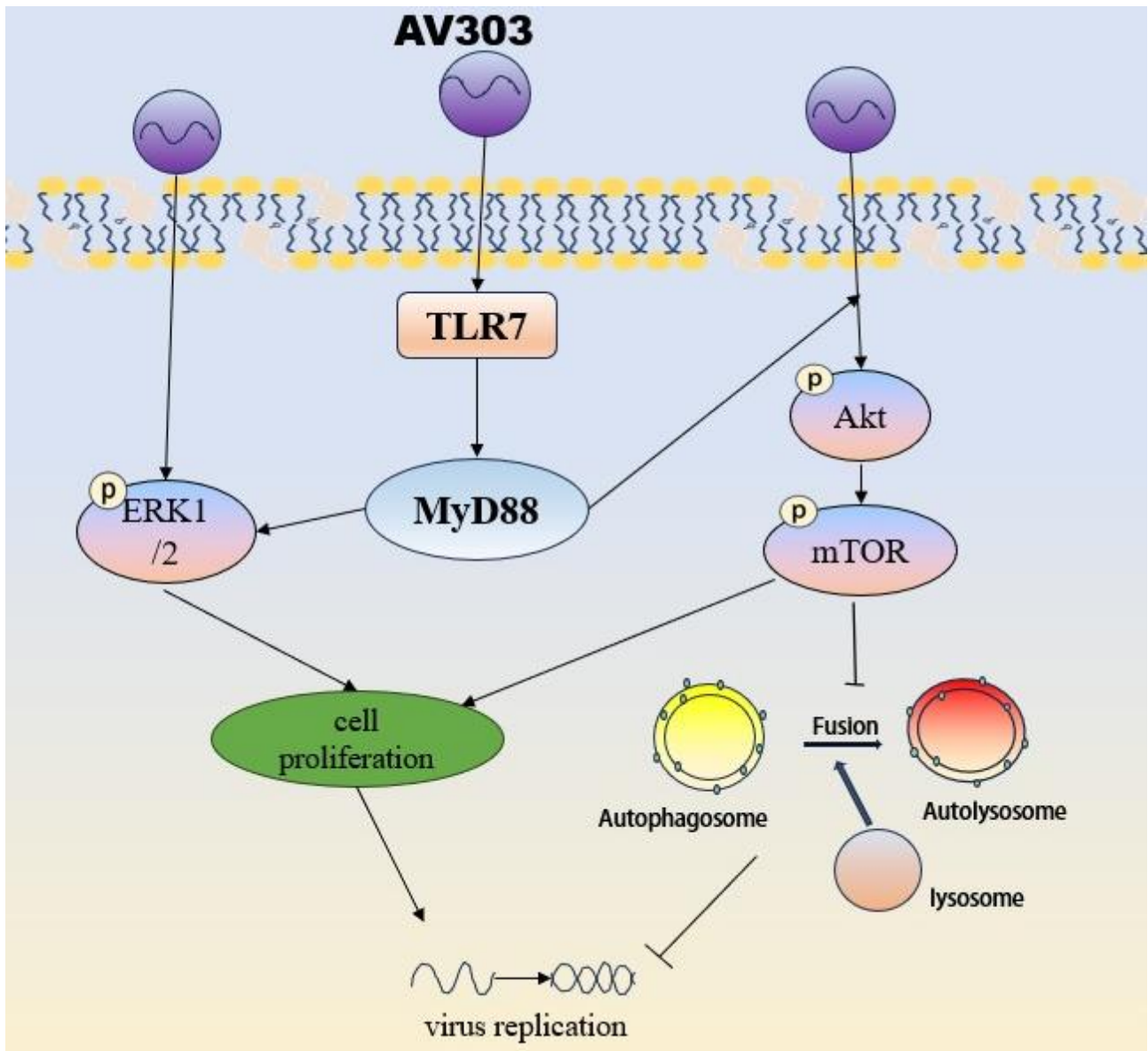


Fig. 6: MyD88 mediates AV303 induced autophagy and cell proliferation to achieve self-replication model.

Previous studies have shown that CP and NCP BVDV strains can initiate cellular autophagy. In this study, we still observed that NCP BVDV AV303 can induce autophagy initiation in cells, but the degradation stage of autophagy initiated by AV303 was blocked, indicating impaired autophagy flux. This process is similar to that of Dengue virus (Metz *et al.*, 2015), which achieves self-replication by inhibiting autophagy flux and relies on p62 receptor mediated protease degradation. There is growing evidence that the active state of autophagy can affect the immune system (Virgin and Levine, 2009; Metur and Klionsky, 2021). The replication of AV303 is closely related to autophagic activity, and the use of autophagic drugs reverse regulates the replication ability of AV303. Therefore, the replication ability of AV303 is closely related to its capacity for autophagic flux. When autophagy is significantly inhibited, the replication ability of the AV303 virus is enhanced, and vice versa.

Viruses are specialized intracellular parasites that rely on nutrients and energy within cells for their survival, and their replication relies on cellular raw materials, especially nucleic acids and proteins (Cvirkaite-Krupovic *et al.*,

2015; Goodwin *et al.*, 2015; Strating and van Kuppeveld, 2017). As a foreign substance, NCP BVDV can still be sensed after invading host cells. Previous research has shown that after NCP BVDV infection the viability of infected cells was significantly greater than that of normal cells (Shin *et al.*, 2023; Li *et al.*, 2024). This abnormal phenomenon may indicate that BVDV has evolved the ability to hijack host cell processes.

Our research further investigated cell proliferation after infection. After AV303 infection, the cells proliferated more efficiently, which also indicated that the virus had a greater chance of replicating. We tested two classical pathways related to cell proliferation, the Akt/mTOR and ERK pathways, which were previously shown to be closely related to cell proliferation. Akt/mTOR activation promotes cell proliferation (Glaviano *et al.*, 2023), and the activity of ERK can mediate different antiapoptotic events (Sugiura *et al.*, 2021). Research has found that Akt/mTOR is involved in the replication of many viruses. Firstly, it was found that many DNA viruses can activate this pathway to avoid many stress signals (Buchkovich *et al.*, 2008). In

addition, RNA viruses have evolved this mechanism, such as hepatitis C virus (HCV), which promotes cell survival and establishes sustained infection by activating Akt/mTOR (Mannová and Beretta, 2005). NDV upregulates the host cap dependent translation mechanism by activating the Akt/mTOR pathway, which is beneficial for viral protein synthesis (Zhan *et al.*, 2020). Additionally, one study revealed the relationship between these two cell types of viral strains and ERK, with the CP type activating the ERK pathway but the NCP type not doing so (Yamane *et al.*, 2009). However, we found that ERK1/2 can be activated by the AV303 virus strain (NCP BVDV) in MDBK. The ERK pathway is not only involved in the differentiation and activation of immune cells but also regulates the immune response, which both promotes and prevents over immunity in the immune system (Lucas *et al.*, 2022). In addition, detection of the Akt/mTOR pathway revealed that the degree of phosphorylation of Akt still increased while the phosphorylation of mTOR activity has no significant difference after MyD88 was knocked down. The Akt/mTOR signaling pathway is not only a pathway that promotes cell proliferation, but also an important pathway that regulates autophagy. When mTOR phosphorylation is enhanced, autophagy will be inhibited. In our study, after knocking down the MyD88 gene, Akt/mTOR signaling transduction was abnormal, and autophagy flow stability was restored. In this case, we believe that this is a new strategy for AV303 to evade immunity.

Innate immunity plays an important role in the host's fight against viral infection and invasion, with IFN-I being the core molecule in combating viral infections. However, there has been no consensus on the effect of NCP BVDV on IFN-I for a long time. This may arise from variations in the effects of different strains or differences in virulence within the same strain (Quintana *et al.*, 2020). It is precisely because of the adaptive nature of BVDV that it is urgently necessary to study its interaction with the host. This study investigated the immune evasion strategy of AV303 through interactions between viruses and cells. Clarifying the evasion strategy of the virus will aid in the development of vaccines and drugs. This study revealed that MyD88 can mediate the regulation of host cell autophagy and proliferation by AV303, thereby aiding in its replication (Fig. 6). These findings suggest the potential of MyD88 as a molecular target for anti-BVDV drugs.

Conclusions: In conclusion, our results preliminarily revealed the important role of MyD88 in the replication of NCP BVDV in cells, revealing that NCP BVDV-induced autophagy and proliferation are beneficial for replication.

Authors contribution: KW and YH conducted experiments and data analysis, JX analyzed the data, and YyZ and YjC conducted review and supervision. JY conceptualized and reviewed this study, XbL provided funding and instruments for the study. All authors interpreted the data, critically revised the manuscript for important intellectual contents and approved the final version.

REFERENCES

- Buchkovich NJ, Yu Y, Zampieri CA, *et al.*, 2008. The TORrid affairs of viruses: effects of mammalian DNA viruses on the PI3K–Akt–mTOR signalling pathway. *Nat Rev Microbiol* 6(4):266-275.
- Chang J, Burkett PR, Borges CM, *et al.*, 2013. MyD88 is essential to sustain mTOR activation necessary to promote T helper 17 cell proliferation by linking IL-1 and IL-23 signaling. *Proc. Nat Acad Sci* 110(6):2270-2275.
- Cho D, Mier JW and Atkins MB, 2009. PI3K/Akt/mTOR pathway: a growth and proliferation pathway. *RCC: Mol Targ Clin App* 2009:267-285.
- Cvirkaite-Krupovic V, Carballido-López R and Tavares P, 2015. Virus evolution toward limited dependence on nonessential functions of the host: the case of bacteriophage SPPI. *Virol J* 89(5):2875-2883.
- Delgado M and Deretic V, 2009. Toll-like receptors in control of immunological autophagy. *Cell Death Differ* 16(7):976-983.
- Duan H, Ma Z, Xu L, *et al.*, 2020. A novel intracellularly expressed NS5B-specific nanobody suppresses bovine viral diarrhoea virus replication. *Vet Microbiol* 240:108449.
- Fu Q, Shi H, Zhang H, *et al.*, 2014. Autophagy during early stages contributes to bovine viral diarrhoea virus replication in MDBK cells. *J Basic Microbiol* 54(10):1044-1052.
- Glaviano A, Foo AS, Lam HY, *et al.*, 2023. PI3K/AKT/mTOR signaling transduction pathway and targeted therapies in cancer. *Mol Cancer* 22(1):138.
- Gong Y, Tang N, Liu P, *et al.*, 2022. Newcastle disease virus degrades SIRT3 via PINK1-PRKN-dependent mitophagy to reprogram energy metabolism in infected cells. *Autophagy* 18(7):1503-1521.
- Goodwin CM, Xu S and Munger J, 2015. Stealing the keys to the kitchen: viral manipulation of the host cell metabolic network. *Trends Microbiol* 23(12):789-798.
- Guasparri I, Bubman D and Cesarman E, 2008. EBV LMP2A affects LMP1-mediated NF- κ B signaling and survival of lymphoma cells by regulating TRAF2 expression. *Blood, J Amer Soc Hema* 111(7):3813-3820.
- Iwasaki A, 2007. Role of autophagy in innate viral recognition. *Autophagy* 3(4):354-356.
- Jiang H, Kan X, Ding C, *et al.*, 2022. The multi-faceted role of autophagy during animal virus infection. *Front Cell Infect Microbiol* 12:858953.
- Kader M, Alaoui-EL-Azher M, Vorhauer J, *et al.*, 2017. MyD88-dependent inflammasome activation and autophagy inhibition contributes to Ehrlichia-induced liver injury and toxic shock. *PLoS Pathog* 13(10):e1006644.
- Li D, Zhang J, Yang W, Li P, *et al.*, 2021. African swine fever virus protein MGF-505-7R promotes virulence and pathogenesis by inhibiting JAK1- and JAK2-mediated signaling. *J Bio Chem* 297(5).
- Li W, Li H, Liu Y, *et al.*, 2012. New variants of porcine epidemic diarrhoea virus, China, 2011. *Emerg Infect Dis* 18(8):1350.
- Li Z, Zhang Y, Zhao B, *et al.*, 2024. Non-cytopathic bovine viral diarrhoea virus (BVDV) inhibits innate immune responses via induction of mitophagy. *Vet Res* 55(1):1-18.
- Lindberg A and Houe H, 2005. Characteristics in the epidemiology of bovine viral diarrhoea virus (BVDV) of relevance to control. *Prev Vet Med* 72(1-2):55-73.
- Liu JH, Chen C, Li ZY, *et al.*, 2020. The MyD88 inhibitor TJ-M2010-2 suppresses proliferation, migration and invasion of breast cancer cells by regulating MyD88/GSK-3 β and MyD88/NF- κ B signalling pathways. *Exp. Cell Res* 394(2):112157.
- Liu X, Nawaz Z, Guo C, *et al.*, 2022. Rabies virus exploits cytoskeleton network to cause early disease progression and cellular dysfunction. *Front Vet Sci* 9:889873.
- Lucas RM, Luo L and Stow JL, 2022. ERK1/2 in immune signalling. *Biochem. Soc. Trans* 50(5):1341-1352.
- Luo Y, Liu Y, Wang C, *et al.*, 2021. Signaling pathways of EBV-induced oncogenesis. *Cancer Cell Int* 21(1):93.
- Ma Y, Wang L, Jiang X, *et al.*, 2022. Integrative transcriptomics and proteomics analysis provide a deep insight into bovine viral diarrhoea virus-host interactions during BVDV infection. *Front Immunol* 13:862828.
- Mannová P and Beretta L, 2005. Activation of the N-Ras–PI3K–Akt–mTOR pathway by hepatitis C virus: control of cell survival and viral replication. *Virol J* 79(14):8742-8749.
- Mathew R, Karantza-Wadsworth V and White E, 2007. Role of autophagy in cancer. *Nat Rev Cancer* 7(12):961-967.

- McCance DJ, 2005. Human papillomaviruses and cell signaling. *Science's STKE* 2005(288):e29.
- Metur SP and Klionsky DJ, 2021. Adaptive immunity at the crossroads of autophagy and metabolism. *Cell Mol Immunol* 18(5):1096-1105.
- Metz P, Chiramel A, Chatel-Chaix L, et al., 2015. Dengue virus inhibition of autophagic flux and dependency of viral replication on proteasomal degradation of the autophagy receptor p62. *Virol J* 89(15):8026-8041.
- Mirosław P, Rola-Łuszczak M, Kuźmak J, et al., 2022. Transcriptomic analysis of MDBK cells infected with cytopathic and non-cytopathic strains of bovine viral diarrhoea virus (BVDV). *J Viruses* 14(6):1276.
- Nojima H, Adachi M, Matsui T, et al., (2008). IQGAP3 regulates cell proliferation through the Ras/ERK signalling cascade. *Nat Cell Biol* 10(8):971-978.
- Ogrodnik M, 2021. Cellular aging beyond cellular senescence: Markers of senescence prior to cell cycle arrest in vitro and in vivo. *Aging Cell* 20(4):e13338.
- Pang F, Long Q and Wei M, 2023. Immune evasion strategies of bovine viral diarrhoea virus. *Front. Cell Infect Microbiol* 13:1282526.
- Parzych KR and Klionsky DJ, 2014. An overview of autophagy: morphology, mechanism, and regulation. *Antioxid Redox Signal* 20(3):460-473.
- Peterhans E, Bachofen C, Stalder H, et al., 2010. Cytopathic bovine viral diarrhoea viruses (BVDV): emerging pestiviruses doomed to extinction. *Vet.Res* 41(6):44.
- Quintana ME, Barone LJ, Trotta MV, et al., 2020. In-vivo activity of IFN- λ and IFN- α against bovine-viral-diarrhoea virus in a mouse model. *FrontVet Sci* 7:45.
- Rajput MK, Abdelsalam K, Darweesh MF, et al., 2017. Both cytopathic and non-cytopathic bovine viral diarrhoea virus (BVDV) induced autophagy at a similar rate. *Vet Immunol Immunopathol* 193:1-9.
- Rubio RM and Mohr I, 2019. Inhibition of ULK1 and Beclin1 by an α -herpesvirus Akt-like Ser/Thr kinase limits autophagy to stimulate virus replication. *Proc Natl Acad Sci USA* 116(52):26941-26950.
- Salcedo R, Cataisson C, Hasan U, et al., 2013. MyD88 and its divergent toll in carcinogenesis. *Trends Immunol* 34(8):379-389.
- Senkevich TG, Yutin N, Wolf YI, et al., 2021. Ancient gene capture and recent gene loss shape the evolution of orthopoxvirus-host interaction genes. *MBio* 12:e01495-21.
- Shi CS and Kehrl JH, 2008. MyD88 and Trif target Beclin 1 to trigger autophagy in macrophages. *J Biol Chem* 283(48):33175-33182.
- Shin SU, Han DG, Cho HC, et al., 2023. Non-cytopathic bovine viral diarrhoea virus 2 induces autophagy to enhance its replication. *Vet Med Sci* 9(1):405-416.
- Siracusano G, Venuti A, Lombardo D, et al., 2016. Early activation of MyD88-mediated autophagy sustains HSV-1 replication in human monocytic THP-1 cells. *Sci Rep* 6(1):31302.
- Song J, Li Y, Wu K, et al., 2024. MyD88 and Its Inhibitors in Cancer: Prospects and Challenges. *Biomolecules* 14(5):562.
- Spence RA, Kati WM, Anderson KS, et al., 1995. Mechanism of inhibition of HIV-1 reverse transcriptase by nonnucleoside inhibitors. *Science* 267(5200):988-993.
- Steinbach A and Riemer AB, 2018. Immune evasion mechanisms of human papillomavirus: An update. *Inter J Cancer* 142(2):224-229.
- Strating JR and van Kuppeveld FJ, 2017. Viral rewiring of cellular lipid metabolism to create membranous replication compartments. *Curr Opin Cell Biol* 47:24-33.
- Sugiura R, Satoh R and Takasaki T, 2021. ERK: a double-edged sword in cancer. ERK-dependent apoptosis as a potential therapeutic strategy for cancer. *Cells* 10(10):2509.
- Thompson JM and Iwasaki A, 2008. Toll-like receptors regulation of viral infection and disease. *Adv Drug Deliv Rev* 60(7):786-794.
- Tognarelli EI, Palomino TF, Corrales N, et al., 2019. Herpes simplex virus evasion of early host antiviral responses. *Front Cell Infect Microbiol* 9:127.
- Urcuqui-Inchima S, Cabrera J and Haenni AL, 2017. Interplay between dengue virus and Toll-like receptors, RIG-I/MDA5 and microRNAs: Implications for pathogenesis. *Antiviral Res* 147:47-57.
- Virgin HW and Levine B, 2009. Autophagy genes in immunity. *Nat Immunol* 0(5):461-470.
- Wang W, Zhou Z, Xiao X, et al., 2021. SARS-CoV-2 nsp12 attenuates type I interferon production by inhibiting IRF3 nuclear translocation. *Cellul Mol Immunol* 18(4):945-953.
- Wang Y, Li Y, Zhang T, et al., 2018. Genistein and Myd88 activate autophagy in high glucose-induced renal podocytes in vitro. *Med Sci Monit* 24:4823.
- Xu Y, Liu XD, Gong X, et al., (2008). Signaling pathway of autophagy associated with innate immunity. *Autophagy* 4(1):110-112.
- Yamane D, Zahoor MA, Mohamed YM, et al., 2009. Activation of extracellular signal-regulated kinase in MDBK cells infected with bovine viral diarrhoea virus. *Arch Virol* 154(9):1499-1503.
- Zhan Y, Yu S, Yang S, et al., 2020. Newcastle Disease virus infection activates PI3K/Akt/mTOR and p38 MAPK/Mnk1 pathways to benefit viral mRNA translation via interaction of the viral NP protein and host eIF4E. *PLoS Pathog* 16(6):e1008610.
- Zhang ZY, Bao XL, Cong YY, et al., 2020. Autophagy in age-related macular degeneration: A regulatory mechanism of oxidative stress. *Oxid Med Cell Longev* 2020(1):2896036.
- Zheng L, Wang X, Guo D, et al., 2021. Porcine epidemic diarrhoea virus E protein suppresses RIG-I signaling-mediated interferon- β production. *Vet Microbiol* 254:108994.
- Zost SJ, Wu NC, Hensley SE, et al., 2019. Immunodominance and antigenic variation of influenza virus hemagglutinin: implications for design of universal vaccine immunogens. *J Infect Dis* 219 (Supplement_1):S38-S45.